Characterisation of multi-layer InAs/InP quantum wires by surface photovoltage and photoluminescence spectroscopies

2010 J. Phys.: Conf. Ser. 253 012043

(http://iopscience.iop.org/1742-6596/253/1/012043)

Journal of Physics: Conference Series **253** (2010) 012043 doi:10.1088/1742-6596/253/1/012043

Characterisation of multi-layer InAs/InP quantum wires by surface photovoltage and photoluminescence spectroscopies

Ts Ivanov[1], V Donchev[1], T Angelova[2], A Cros[2], A Cantarero[2], N Shtinkov[3], K Borissov[1], D Fuster[4], Y González[4] and L González[4]

[1] Faculty of Physics, Sofia University, 5, blvd. J. Bourchier, Sofia-1164, BULGARIA
[2] Institut de Ciència dels Materials, Univ. de València, P.O. Box 22085E-46071, València, SPAIN
[3] Department of Physics, University of Ottawa, Ottawa ON, CANADA K1N 6N5
[4] Instituto de Microélectronica de Madrid (CNM- CSIC), Isaac Newton 8, Tres Cantos, 28760, Madrid, SPAIN

Corresponding author: tsvetanivanov@lycos.com

Abstract. The optical properties of multi-layer InAs/InP quantum wires (QWRs) with two different spacer thicknesses have been investigated by means of room temperature surface photovoltage (SPV) and photoluminescence (PL) spectroscopies, combined with empirical tight binding electronic structure calculations and structural data. The SPV and PL spectra reveal several features, which energy positions are in good agreement. They have been ascribed to excitonic transitions, which take place in the QWR families with heights differing by an integer number of monolayers. Comparing the experimental results with the theoretical ones, we have estimated the QWR family heights and the average atomic concentration of phosphorus in the QWRs. From the simultaneous analysis of the SPV amplitude and phase spectra, based on our vector model for SPV signal representation, a deeper understanding of the SPV results and of the mechanisms of carrier separation in the sample is obtained.

1. Introduction

The interest in multi-layers of self-assembled InAs/InP quantum wires (QWRs) grown in the Stranski-Krastanov mode is motivated by their promising applications in light emitting devices in the 1.3 - 1.55 μm wavelength range used in optical fibre telecommunications [1]. The optical properties of these nanostructures have been studied by means of low-temperature photoluminescence (PL) spectroscopy, combined with electronic structure calculations in frames of the envelope function approximation. The PL spectra have revealed several wide bands, which have been generally attributed to emission of QWRs belonging to different families with heights differing by an integer number of monolayers (MLs) [2-5]. There are relatively few experimental investigations at room temperature (RT), which will be the operating temperature of a final device, based on the discussed multi-layers [6-8]. Due to its high sensitivity even at RT, the surface photovoltage (SPV) spectroscopy is an alternative to avoid the difficulties related to optical absorption measurements in nanostructures [9-11].

In this work we apply SPV spectroscopy to study multi-layer InAs/InP QWRs at RT in combination with PL measurements, structural data from previous studies [3], and comparison with empirical tight binding (ETB) electronic structure calculations.

2. Experimental and calculation details

Two samples were grown on (001) semi-insulating (SI) InP:Fe substrates by solid-source molecular beam epitaxy. They contain a 150 nm InP buffer layer and a stack of seven InAs QWR layers, separated by InP spacers of thickness d = 10 and 20 nm in the two samples. The growth temperature was 515°C and 380°C for the QWRs and the InP spacers, respectively (figure 1). High resolution transmission electron microscopy (TEM) [3] has shown that the QWRs are oriented along [1-10] and their average height H and lateral width are around 3.2 nm and 10.3 nm, respectively. The residual doping in the buffer and the QWR structure is n-type, of the order of 1×10^{17} cm^{-3}.

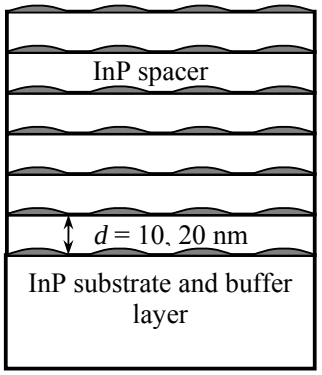

Figure 1. Scheme of the samples.

Details about the set-up used for SPV spectral measurements in metal-insulator-semiconductor operation mode and the measurement procedure can be found elsewhere [10, 12]. Here the semitransparent probe electrode was a SnO_2 film deposited on a quartz glass. It was adjusted to gently press the sample to a grounded copper platform. All measurements were performed with normal incident light chopped at 94Hz, keeping a constant photon flux density ($\Phi \approx 1.5\times10^{14}$ cm^{-2}s^{-1} ± 2%) for all wavelengths, scanned from high towards low ones. The PL spectra were measured at RT using an Ar+ ion laser (514.5 nm line) a 0.19 TRIAX single monochromator (600 grooves/mm grating) and a N_2-cooled InGaAs detector connected to a lock-in amplifier.

The procedure for the ETB electronic structure calculations is described in detail in [13]. The intermixing that inevitably exists in such structures was taken into account by considering a nonzero phosphorus concentration [P] in the QWR, because this method is consistent with experimental observations for the InAs/InP system [13]. Since InAs/InP QWRs and dots are relatively flat, the effect of the lateral confinement on the transition energies is small [13] and was therefore neglected in our calculations. A temperature correction of 65 meV is subtracted from the calculated (at 0K) energies to account for the InAs band gap decrease between 0 and 300K [14].

3. Results and discussion

The SPV amplitude spectra of the samples with d = 10 and 20 nm, respectively, are shown on figures 2(a) and 2(b). In the energy range 0.75–0.9 eV they reveal a few steps or peaks superimposed on a smooth background. The PL spectra, given on the same figures, represent broad bands, which can be decomposed to a few Gaussians. The energy positions (in eV) of the SPV (PL) features for the sample with d = 10 nm are: 0.84 (0.83); 0.81 (0.80); 0.77 (0.77) and (0.72), while for the sample with d = 20 nm they are: 0.85 (0.84); 0.81 (0.81) and (0.78); the lowest-energy peaks are absent in the SPV spectra. The good agreement between the SPV and PL features implies that they originate from electronic transitions between the same electronic states in the samples. We have checked that these features are absent in the PL spectrum of bulk InP. Thus, in accordance with our previous works on PL spectroscopy of InAs/InP QWRs [2-4, 8], we can also ascribe the SPV features to excitonic transitions arising in QWR families with heights differing by an integer number of MLs. The small difference of ~ 10 meV between the SPV and PL peak positions represents the Stokes shift for the QWR exciton.

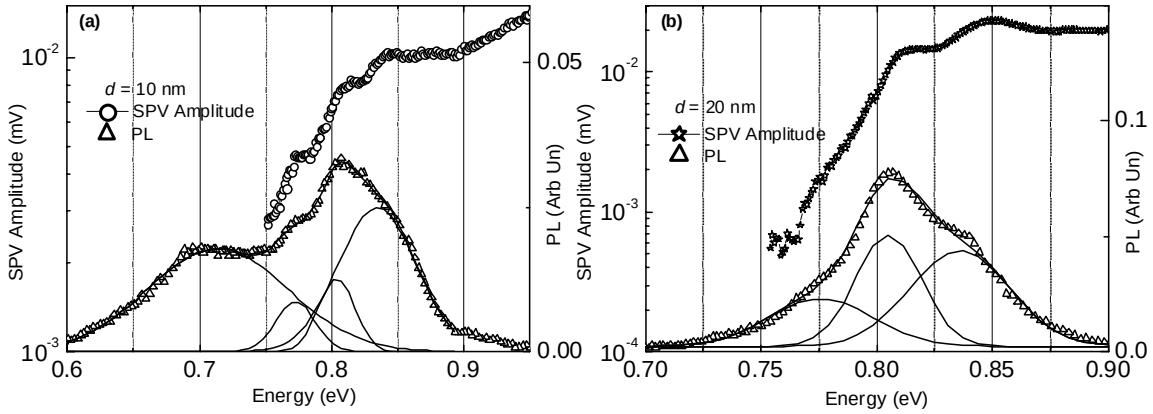

Figure 2. SPV amplitude and PL spectra of the samples with d = 10 (a) and 20 nm (b). The PL band is decomposed to Gaussians.

In order to determine the QWR family heights we have compared the experimental results with numerical calculations of the electronic structure performed by the ETB method. The calculated transition energies for different QWR heights as a function of [P] are shown with solid lines in figure 3. The horizontal dashed lines in the same figure represent the experimental peak energies for both samples. From the multiple intersections of the two line sets we have selected the ones giving the best agreement. The procedure is described and verified in [13]; it requires that i) H increase by 1 ML between peaks and ii) [P] remain nearly constant for the different QWR families. Hence, the results suggest that the peaks around 0.85, 0.81 and 0.77 eV originate form QWR families with heights 7, 8 and 9 MLs, respectively.

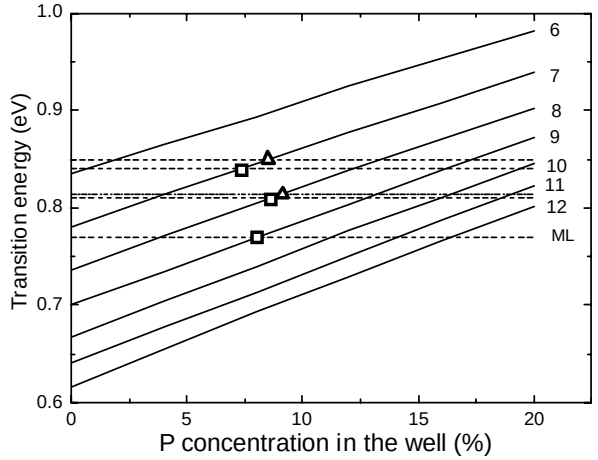

Figure 3. Transition energies of a single InAsP/InP QWR as a function of the P content for QWRs heights from 6 to 12 MLs. The dashed lines show the SPV peak values and their relevant intersections with the calculated curves are illustrated by squares (d = 10 nm) and triangles (d = 20 nm).

The PL peak with the lowest energy (0.72 eV) in the sample with d = 10 nm is much broader and could account for a number of families (with heights 10-12 ML). Alternatively, this emission could originate from larger QWRs formed by the overlapping of two or more small wires. Such wires have been observed by atomic-scale cross-sectional scanning tunneling microscopy [15].

The intersections of the curves in figure 3 show also that a constant P concentration in the QWRs of the order of 8 % can effectively represent the effects of the InAs/InP intermixing on the optical transition energies. The error in [P] can be estimated to ± 4% and it results from the uncertainty in the

InAs/InP valence band offset (0.3-0.4 eV), which gives an error of ±(2-3)% [13], the experimental error in the transition energies (±5 meV) giving ±0.6% and the effect of the strain relaxation during the QWR formation (< 1% [13]) which is not taken into account in the calculations.

Similar samples with InP spacer layers, grown at higher temperatures (515°C), have been investigated in our previous study [8]. The comparison with the present results shows that the current QWRs are higher, but have a lower equivalent P concentration. This height difference is supported by the TEM results [3]. It is explained by the fact that at higher growth temperature of the InP spacers an enhanced P/As exchange takes place, which favours the formation of lower InAs wires with smaller cross section aspect ratio, as pointed out in [3]. The lower equivalent P concentration obtained for the present QWRs corresponds with their less efficient P/As exchange and larger cross section aspect ratio.

The slight difference in peak positions between the samples with d = 20 nm and d = 10 nm is probably due to the increase of the electron coupling between adjacent layers with decreasing d, as discussed in [4].

In order to obtain a deeper understanding of the SPV results and to study the mechanisms of carrier separation necessary for the SPV signal formation, we analyze in parallel the SPV amplitude and phase spectra shown on figure 4. For that purpose we have used our vector model [11], in which the SPV signal is represented by a radial vector, with magnitude equal to the SPV amplitude and angle with respect to the X-axis equal to the SPV phase. The occurrence of more than one SPV process is then represented by summation of the corresponding SPV vectors.

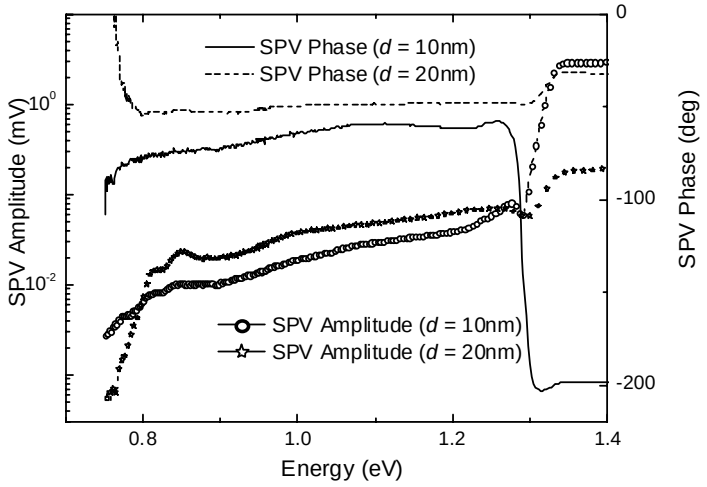

Figure 4. SPV amplitude and phase spectra of both samples in the whole spectral range under study.

In the range 0.75 – 0.9 eV, where the QWR spectral features are observed in the PL and SPV amplitude spectra, the SPV phase is in IV^{-th} quadrant (see figure 4). This indicates an upward energy band bending in the region of the QWR structure with respect to the bulk [10, 11]. In fact an upward band bending at the sample surface is expected because of the n-type residual doping of the multi-layer structure and buffer layer. The QWR structure is then situated in the space charge region (SCR), which arises at the sample surface with a built-in electric field [see figure 5(b)]. The SPV signal from the QWRs is due to photocarriers, which thermally escape from the InAs potential wells into the InP barriers, where they are separated by the SCR built-in electric field. Since the carrier escape is easier for higher energy states, the SPV peaks at higher energies are stronger. Thus, the SPV spectra extend the information obtained by PL, where the lowest energy transition is predominantly observed. For energies from 0.9 to 1.27 eV the SPV phase remains nearly constant, while the amplitude smoothly increases, which suggests that in this range the optical absorption is associated with excited states in the multilayer structure.

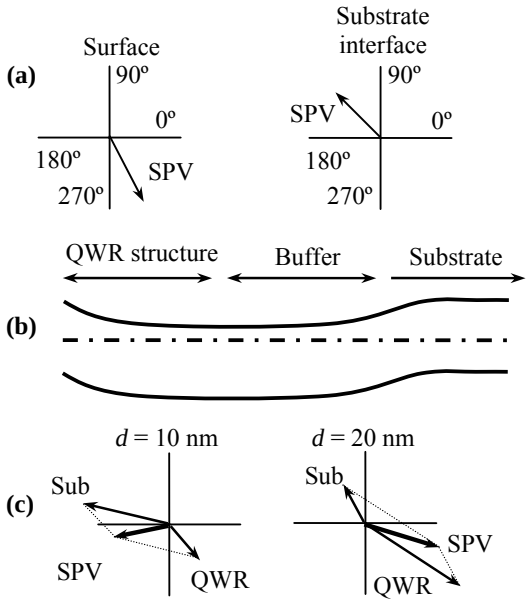

Figure 5. SPV vectors for both interfaces (a); alignment of the energy bands (b); summation of the SPV vectors of the substrate (Sub) and of the multilayer structure (QWR) for both samples (c)

At higher energies the SPV amplitude spectrum for both samples reveals a minimum around 1.29 eV followed by a strong step in the range 1.29 - 1.34 eV. In the same energy range a jump occurs in the SPV phase spectrum. The step is associated with band to band absorption in InP (bandgap energy 1.34 eV). The amplitude minimum and the phase jump at 1.29 eV can be explained taking into account the nearly opposite phases of the SPV signals from the multilayer structure and from the bulk InP. The first one includes the signals from the InP spacer layers and from excited states in the InAs QWRs. The phase in this case is in IV^{-th} quadrant due to the upward energy band bending, as explained above. The second one includes the signal from the interface buffer/substrate, where the band bending is downward with respect to the bulk, because of the different layouts of the Fermi levels in the two materials [n-type InP buffer and SI InP substrate, see figure 5(b)]. Therefore, the SPV signal associated with the band to band absorption in the bulk InP is represented by a vector in II^{-nd} quadrant (vector Sub) [10, 11], contrary to the SPV vector of the multilayer structure (vector QWR).

The superposition of the SPV signals from the multilayer structure and from the bulk InP is represented in figure 5(c) by summation of two SPV vectors nearly opposite in orientation (vector QWR in IV^{-th} and vector Sub in II^{-nd} quadrant). It is easy to understand that this superposition leads to a minimum in the SPV amplitude and a SPV phase jump, as observed around 1.29 eV. The different strength and direction of the SPV phase jump for the two samples can be explained by different orientation and magnitude of these sets of vectors. In the case of the sample with d = 10 nm, where the multilayer structure is thinner, the bulk InP vector is relatively strong as compared to the multilayer vector and forms an obtuse angle with it, as shown in figure 5(c) left. The growth of vector Sub leads to clockwise rotation of the overall SPV vector across III^{-rd} quadrant. The bulk InP vector of the sample with d = 20 nm, where the multilayer structure is thicker, is relatively weak as compared to the multilayer vector and forms an obtuse angle with it, as shown in figure 5(c) right. Therefore the growth of vector Sub in this case leads only to a small anticlockwise rotation of the overall SPV vector and an initial SPV amplitude minimum at 1.29 eV. The following increase in the SPV amplitude is due to the increased contribution of the InP spacer layers [the QWR vector in figure 5(c) right].

4. Conclusion

We present a comparative study of the optical absorption and emission of multi-layer InAs/InP QWRs, performed by RT SPV and PL spectroscopies in combination with ETB calculations and structural data obtained in previous studies. The energies of the numerous features in the SPV spectra are in

good agreement with the ones observed in PL. They are interpreted as due to excitonic transitions, which arise in QWR families with different heights. The values of the later (7, 8 and 9 MLs) are estimated from the comparison of the experimental and the calculated transition energies. Using this comparison we have found also that the degree of P intermixing in the wires is equivalent to a constant P concentration of the order of 8%.

The dependence of the QWR height on the growth temperature of the InP spacer layers is discussed and explained by the corresponding temperature dependent behaviour of the P/As exchange processes.

Due to the residual n-type doping of the QWR structure and buffer layer, the energy bands are bent upward (downward) at the sample surface (at the interface buffer/substrate), which results in non-trivial features in the SPV spectrum, which have been successfully explained with the help of our vector model for SPV signal representation.

Finally, it should be noted that this study demonstrates the abilities of the SPV spectroscopy for characterization of complex nanostructures at RT.

Acknowledgements
This work was supported by the Sofia University research fund (contract 149/2010), Ministry of Education and Science of Spain (MAT2009-10350, FEDER) and the Alexander von Humboldt Foundation. The authors would like to thank assoc. prof. Germanova for the critical reading and fruitful discussions.

References

[1] Schwertberger R, Gold D, Reithmaier J P and Forchel A 2003 *J. Crystal Growth* **251** 248–252
[2] Alen B, Martínez-Pastor J, Garcia-Cristobal A, González L and Garcia J M 2001 *Appl. Phys. Lett.* **78** 4025
[3] Fuster D, González M U, González L, González Y, Ben T, Ponce A, Molina S I and Martínez-Pastor J 2004 *Appl. Phys. Lett.* **85** 1424
[4] Fuster D, Martínez-Pastor J, González L and González Y 2006 *J. Phys.* D*: Appl. Phys* **39** 4940
[5] Sidor Y, Partoens B, Peeters F M, Ben T, Ponce A, Sales D L, Molina S I, Fuster D, González L and González Y 2007 *Phys. Rev.* B **75** 125120
[6] Angelova T, Cros A, Cantarero A, Fuster D, González Y and González L 2008 *J. Appl. Phys.* **104** 033523
[7] Mazur Y I, Dorogan V G, Bierwagen O, Tarasov G G, Jr E A D, Noda S, Zhuchenko Z Y, Manasreh M O, Masselink W T and Salamo G J 2009 *Nanotechnology* **20** 065401
[8] Donchev V, Ivanov T, Angelova T, Cros A, Cantarero A, Shtinkov N, Borisov K, Fuster D, González Y and González L 2010 *J. Phys.: Conf. Ser.* **210** 012041
[9] Kronik L and Shapira Y 1999 *Surf. Sci. Rep.* **37** 1
[10] Donchev V, Kirilov K, Ivanov T and Germanova K 2006 *Mat. Sci. & Eng.* B **129** 186
[11] Ivanov T, Donchev V, Germanova K and Kirilov K 2009 *J.Phys.D: App.Phys.* **42** 135302
[12] Ivanov T, Donchev V, Wang Y, Djie H S and Ooi B S 2007 *J. Appl. Phys.* **101** 114309
[13] Dion C, Desjardins P, Shtinkov N, Robertson M D and Schiettekatte F 2008 *Phys. Rev.* B **77** 075338
[14] Fang Z M, Ma K Y, Jaw D H, Cohen R M and Stringfellow G B 1990 *J. Appl. Phys.* **67** 7034
[15] Ulloa J M, Koenraad P M, Fuster D, González L and González Y 2008 *Nanothecnology* **19** 445601